Renewable Energy 36 (2011) 2508–2514

Contents lists available at ScienceDirect

Renewable Energy

journal homepage: www.elsevier.com/locate/renene

Implementation of photovoltaic array MPPT through fixed step predictive control technique

Panagiotis E. Kakosimos*, Antonios G. Kladas

Laboratory of Electrical Machines and Power Electronics, Faculty of Electrical and Computer Engineering, National Technical University of Athens, 9 Iroon Polytechneiou Street, GR 15780 Athens, Greece

ARTICLE INFO

Article history:
Received 22 November 2010
Accepted 28 February 2011
Available online 17 March 2011

Keywords:
Incremental conductance algorithm
Maximum power point tracking
Photovoltaic arrays
Predictive control technique

ABSTRACT

This paper proposes the implementation of Photovoltaic (PV) array Maximum Power Point Tracker (MPPT) through Fixed Step-Model Predictive Controller (FS MPC). The proposed controller scheme is based on the modified INcremental Conductance (INC) algorithm combined with the two-step horizon FS MPC. The current based INC algorithm is subject to major modifications in order to be capable of real time interaction between the MPPT and the controller obtaining sufficient information in one sampling time. The developed technique has been incorporated into a model for the overall simulation of the performance of a PV array for solar energy exploitation and is compared to the conventional approach under solar radiation variation improving PV system utilization efficiency and enabling to optimize system performance. This study also illustrates the effectiveness of the proposed controller scheme under various sky conditions with a simulation model employing real solar radiation data.

1. Introduction

Produced power from photovoltaic (PV) systems can be delivered to the load by the implementation of a DC converter boosting the level of the solar panel output voltage and attaining maximum energy extraction. Forcing the PV system to operate at the Maximum Power Point (MPP) located at the knee of the I–V characteristic constitutes the main target of the controller operating the converter switch. A Maximum Power Point Tracker (MPPT) is also required in order to track the MPP and supply the controller with the appropriate reference input.

One of the most widely used MPPT is the INcremental Conductance (INC) algorithm imposing the reference output to the controller and achieving operation at the maximum power conditions [1,2]. Conventional approach of such an application demands the implementation of a proportional-integral (PI) controller characterized by two main drawbacks, the slow transient response and the possible undesirable oscillations around the MPP. Specifically, PI controller requires sufficient time for the system to reach steady state operation increasing the time interval between two successive reference outputs from the MPPT and hence; deteriorating dynamic performance [3–5].

The interest in this area is significantly growing in researcher communities focusing mainly on the MPPT efficiency improvement. Fuzzy model-based approach [6–8], genetic algorithms [9] and full gradient-based techniques have been enlisted to improve MPPT performance obtaining sufficient information in one sampling time and thus speeding up MPPT operation [10]. However, the possibilities of today's microprocessors facilitate also the implementation of efficient control techniques, achieving significant improvements almost independently of the adopted MPPT algorithm [11]. Such a control technique is the Model Predictive Controller (MPC) employed to solve a finite-horizon optimal control problem at each sampling instant and obtain control actions for both the present time and a future period [12,13].

MPC presents several advantages over the conventional control techniques such as easy implementation and multivariable case consideration [14,15], and is expected to improve PV system utilization efficiency under continuous changes in solar radiation overcoming disturbances and uncertainties [16]. The implementation of a PV array MPPT using MPC combines two keys of vital importance, speed and reliability, avoiding unacceptable oscillations despite the increased speed. The most obvious limitations in these applications are the required computational effort and the quality of the microprocessor [12].

In this paper the implementation of a PV array MPPT through Fixed Step (FS) MPC is presented for first time. The two-step horizon predictive control technique combined with the modified INC algorithm is initially analyzed. A particular methodology is then introduced proposing real time interaction between the MPPT

* Corresponding author.
E-mail address: panoskak@gmail.com (P.E. Kakosimos).

0960-1481/$ – see front matter © 2011 Elsevier Ltd. All rights reserved.
doi:10.1016/j.renene.2011.02.021

and the controller improving system transient response under rapid changes in solar radiation and is compared with the conventional approach. Moreover, this study illustrates the effectiveness of the proposed controller employing real solar radiation data for various sky conditions. Results have shown that the overall system can attain high power conversion efficiency.

2. Overall system configuration

The overall system, as shown in Fig. 1, consists of the main following components: the PV array (A.), which generates power directly from solar radiation, the boost converter (B.), whose switch is operated by the control scheme of the MPPT (F.) and the MPC (G.). Due to the fact that the first priority of the boost converter control is MPP tracking, variations may appear in system output voltage (V_C) and therefore, an inverter AC to DC (D.) is then applied to provide energy to the network with stable voltage.

Control strategy in this study is based on the DC step-up converter boosting the level of the PV system output voltage, as well as determining the factors of maximum power exploitation. PV system output voltage (v_{PV}) and current (i_{PV}) measurements are formed as inputs for the MPPT and the predictive controller. The MPPT reference output current (i^*) and the converter output voltage (v_C) are also designated as inputs for the MPC in order to obtain sufficient information in one sampling time and operate the boost converter switch with the binary output of s. The switch condition is determined by the value of the binary variable of s, which is considered as closed when s is equal to zero; while on the other case is considered as open.

3. Proposed control system analysis

MPPT techniques can be divided into three main categories: lookup table methods, perturbation and observation and, computational methods. For the purpose of comparison and owing to its proven good performance, the INC algorithm classified in perturbation and observation methods, is modified and combined with the proposed predictive control technique and hence; is briefly introduced.

3.1. Modified INC algorithm

Because of being easily implemented the INC algorithm is the traditionally used MPPT technique. The main drawbacks against contemporary methods are that at steady state operation, the reference output varies between neighboring values and that under transient phenomena, is not capable of tracking rapidly the MPP. Fig. 2 shows the block scheme of the modified INC algorithm, where

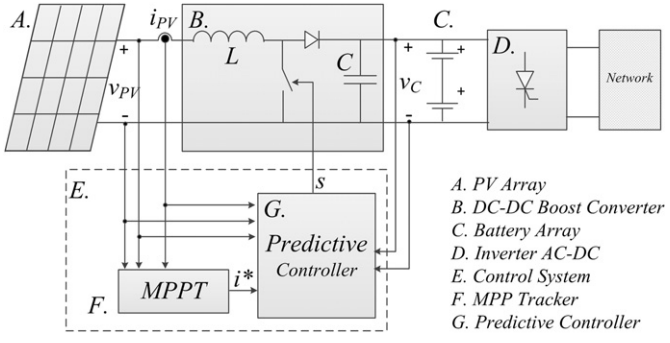

Fig. 1. Simplified schematic of the overall grid connected PV system configuration implementing MPPT through MPC technique.

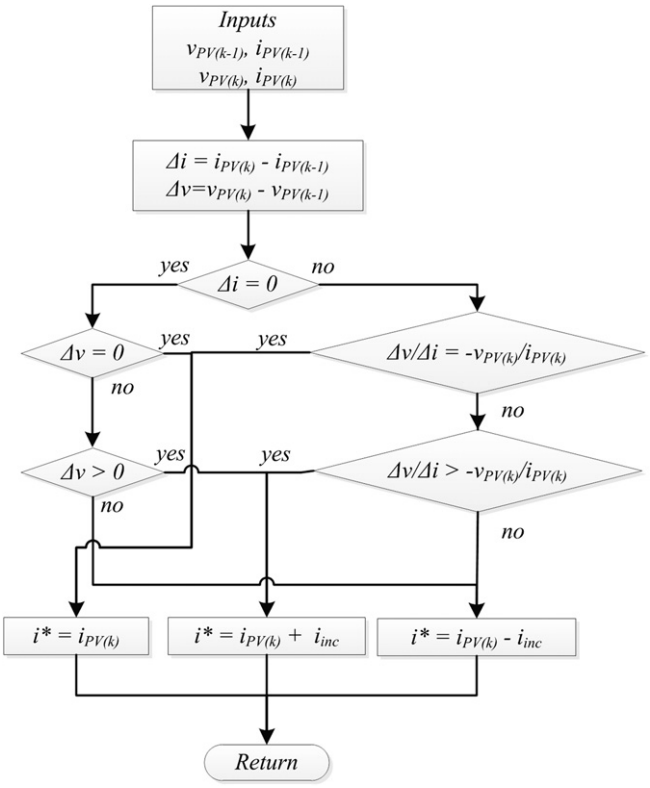

Fig. 2. Block scheme of the modified INC algorithm imposing the reference current i^* to the controller.

time $k-1$ corresponds at the previous sampling time $t-1$, while k indicates the real time measured values.

The INC algorithm is subject to two major modifications. Firstly, the algorithm is modified to impose the reference current to the controller (current based) and secondly, the reference output is defined as the increment of the PV system current measurement ($i_{PV(k)}$), and not as the increment of the previous sampling time reference current ($i^*_{(k-1)}$). The latter modification makes the system capable of deciding rapidly the right direction in P–V curve and following the MPP with larger steps especially during variations.

Tracking the MPP is based on the derivative of the PV system output power (p_{PV}) with respect to the current (i_{PV}). The slope at the MPP is equal to zero determining the desirable operation point:

$$\frac{\partial p_{PV}(v_{PV}, i_{PV})}{\partial i_{PV}} = 0 \rightarrow v_{PV} + i_{PV} \cdot \frac{dv_{PV}}{di_{PV}} = 0 \quad (1)$$

3.2. Predictive controller implementation

The main concept of the FS MPC technique is the prediction of the future behavior of the controlled variables. The criterion of the control method is expressed as a cost function to be minimized. Fig. 3 shows the DC–DC boost converter equivalent circuits for the two conditions of the ideal switch.

When the switch is considered as open, the boost converter operation can be described by the well-known system of equations as follows:

$$\frac{di_{PV}}{dt} = -\frac{1}{L} \cdot i_{PV} + \frac{1}{L} \cdot v_{PV} \quad (2)$$

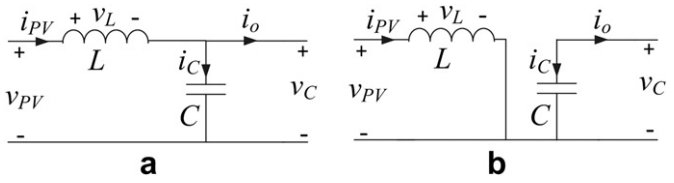

Fig. 3. Boost converter equivalent circuits for the two states of the ideal switch. (a) Open switch, $s = 1$. (b) Closed switch, $s = 0$.

$$\frac{dv_C}{dt} = \frac{1}{C}\cdot i_{PV} + \frac{1}{R\cdot C}\cdot v_c \tag{3}$$

In case of the closed switch, the first order terms vanish and the previous equation system is of the following form:

$$\frac{di_{PV}}{dt} = \frac{1}{L}\cdot v_{PV} \tag{4}$$

$$\frac{dv_C}{dt} = -\frac{1}{R\cdot C}\cdot v_C \tag{5}$$

The discrete time system of equations can derive from (1)–(4) considering the sampling frequency T_s, when the switch is open (5) and (6), or closed (7) and (8).

$$i_{PV(k+1)} = i_{PV(k)} - \frac{T_s}{L}\cdot v_{C(k)} + \frac{T_s}{L}\cdot v_{PV(k)} \tag{6}$$

$$v_{C(k+1)} = \frac{T_s}{C}\cdot i_{PV(k)} + \left(1 - \frac{T_s}{R\cdot C}\right)\cdot v_{C(k)} \tag{7}$$

$$i_{PV(k+1)} = i_{PV(k)} + \frac{T_s}{L}\cdot v_{PV(k)} \tag{8}$$

$$v_{C(k+1)} = \left(1 - \frac{T_s}{R\cdot C}\right)\cdot v_{C(k)} \tag{9}$$

The aforementioned discrete time equation system can be expressed in matrix form as:

$$\begin{bmatrix} i_{PV(k+1)} \\ v_{C(k+1)} \end{bmatrix} = \begin{bmatrix} 1 & -s\cdot\frac{T_s}{L} \\ s\cdot\frac{T_s}{C} & 1 - \frac{T_s}{R\cdot C} \end{bmatrix} \cdot \begin{bmatrix} i_{PV(k)} \\ v_{C(k)} \end{bmatrix} + \begin{bmatrix} \frac{T_s}{L} \\ 0 \end{bmatrix} \cdot v_{PV(k)} \tag{10}$$

Behavior of the controlled variables i_{PV} and v_C can now be predicted for the next sampling instant in order to obtain control actions for both the present time and a future period. One-step horizon predictive controller inputs measured values of i_{PV}, v_{PV}, and v_C estimating future behavior of the controlled variables based on the evaluation of a cost function. Evaluating the chosen cost function two times, for each switch condition, the value of the binary variable s can be computed in order of the predictive controller to decide which one direction in P–V curve must be followed so as to satisfy the applied criteria as shown in Fig. 4.

The determination of the cost function plays a key role in MPC behavior constraining the deviation from the desirable values (i^* and v^*) and can be expressed as:

$$J_{s=n}^{n=0,1} = w_A\cdot\left|v_{C,s=n(k+1)} - v^*\right| + w_B\cdot\left|i_{PV,s=n(k+1)} - i^*\right| \tag{11}$$

where parameters w_A and w_B are in $[1/V]$ and $[1/A]$ units, respectively.

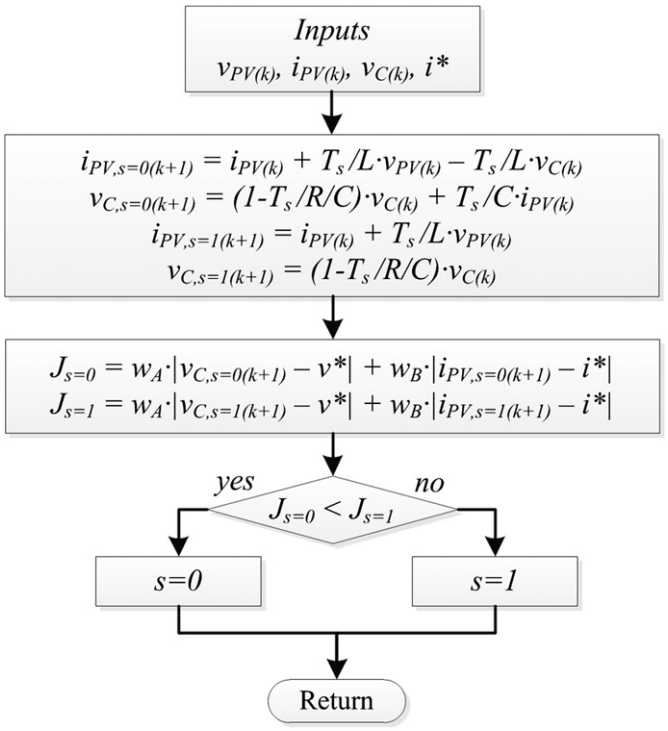

Fig. 4. Block scheme of the MPC technique operating switch state.

Furthermore, MPC technique provides the capacity of predicting system behavior for a future period of n-sampling instants obtaining necessary control actions at present time. Considering n-step horizon MPC is expected to extend system capability of avoiding undesirable oscillations at time $t + n$ because of a variation happened at time t, providing robustness to system behavior.

Discrete time system of equations for the n-step horizon MPC is the following for the two switch conditions, respectively as (6)–(9):

$$i_{PV(k+n+1)} = i_{PV(k+n)} - s\cdot\frac{T_s}{L}\cdot v_{C(k+n)} + \frac{T_s}{L}\cdot v_{PV(k+n)} \tag{12}$$

$$v_{C(k+n+1)} = s\cdot\frac{T_s}{C}\cdot i_{PV(k+n)} + \left(1 - \frac{T_s}{R\cdot C}\right)\cdot v_{C(k+n)} \tag{13}$$

In the case of the two-step horizon MPC the cost function is required to be evaluated four times, for each one combination for the binary variable s at the respective sampling times $t + 1$ and $t + 2$ and has the following form:

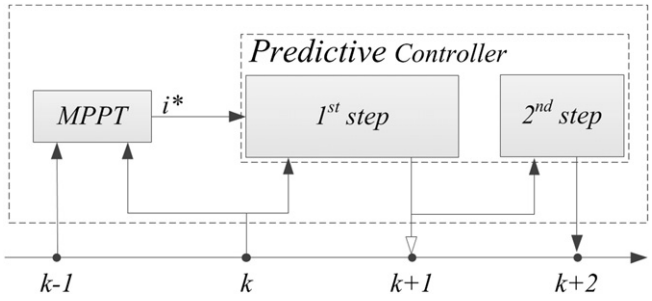

Fig. 5. Time sequence of the interaction between the controller (MPPT, predictive controller) and the controlled system. Time k corresponds to the measured values at the specific sampling instant.

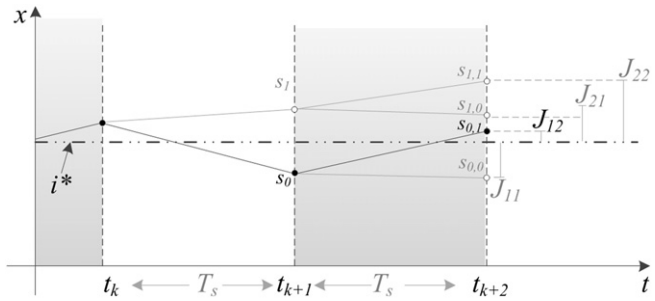

Fig. 6. Schematic diagram of the MPC process for the two-step horizon prediction. The dotted line corresponds to MPPT output, while the black line corresponds to the finally performed actions.

$$J_{s=m}^{n=0,1\&m=0,1} = w_C \cdot \left| v_{C,s=m(k+2)} - v^* \right| + w_D \cdot \left| i_{\mathrm{PV},s=m(k+2)} - i^* \right| + J_{s=n} \tag{14}$$

In order to calculate i_{PV} at time $k+2$ from (12) and (13), there is need to estimate v_{PV} at time $k+1$ for the resultant i_{PV} at the same sampling instant. The output voltage of the PV system can be estimated by using a simplified equivalent equation describing PV system behavior. The PV output voltage (v_{PV}) does not affect significantly controller decision because of the involvement in the equation system for the two switch operations. Avoiding estimation error in the output PV system voltage the cost function at time $k+1$ can play a key role. In (14) the cost function $J_{s=n}$ constitutes a regulator factor depending on the estimation error of the prediction for the output PV voltage at time $k+1$.

Fig. 5 depicts the process of the proposed control scheme for the two-step horizon MPC. MPPT at time k compares the stored values for time $k-1$ with the measured ones saving the recent values, and concurrently, yields and imposes the desirable reference current to the MPC. The latter inputs the measured values and the reference current forcing the PV system to operate with the desirable current at time $k+2$.

Fig. 6 depicts the schematic diagram of the MPC process for the two-step horizon prediction considering only one controlled variable. The dotted line corresponds to the MPPT output, which constitutes the reference current for the controller to follow. At the first step the one-step horizon MPC had to decide between s_0 and s_1, whose difference may not be significant. The two-step horizon MPC decides among s_{00}, s_{01}, s_{10} and s_{11} evaluating the four corresponding cost functions and considering the cost function of the previous step at time $k+1$.

The black line in Fig. 6 corresponds to the finally performed actions indicating the switch state for each step of the prediction.

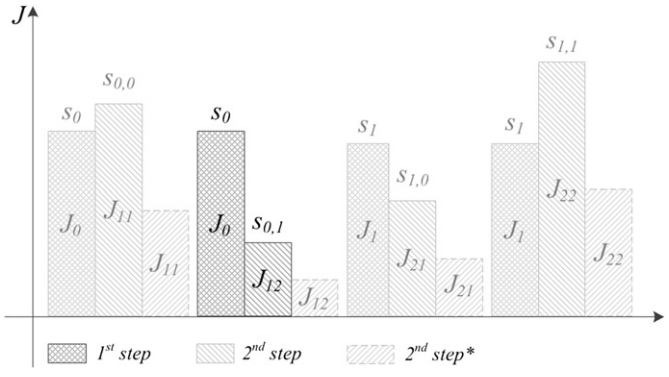

Fig. 7. The four combinations of the switch condition for the two-step horizon MPC and the evaluation of the respective cost functions.

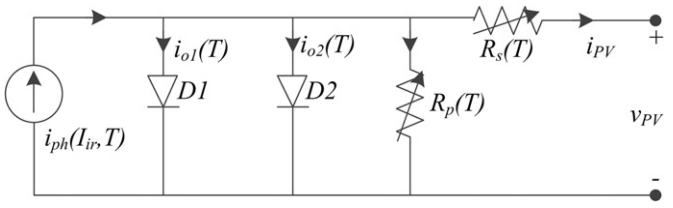

Fig. 8. Equivalent circuit of the solar cell depending on temperature (T) and irradiance values (W/m^2).

Proper configuration of the parameters in the cost function for the two cost functions leads to a robust and stiff system, independent from the estimation error of the non-controlled variables.

Fig. 7 shows the evaluation of the cost function for the two switch conditions and for the two steps of the MPC. Faded colors represent the combinations whose cost function value is higher for the second step than that of the combination with the black color. Considering only the evaluation of the cost function for the second step then the chosen combination may not be the most appropriate depending on the estimation error of the non-controlled variables. Therefore, a combined cost function as in (14) involving the two steps can provide better system response.

Dashed lines in Fig. 7 correspond to the case where the evaluation of the cost function for the second step is taken into consideration with less significance than that of the first step. Depending on the difference between the two evaluated cost functions for the first step the resulting switch condition may differ.

4. Results and discussion

Considering a typical PV system configuration the proposed control technique has been tested under abrupt changes in solar irradiance. In order to illustrate the effectiveness of the introduced control scheme real solar radiation data have been employed for a day with the sporadic presence of clouds.

4.1. PV system configuration

Series and parallel combination of the ideal solar cell model composes the PV array, whose basic mathematical equations are briefly introduced. The equivalent circuit consists of one current source, two exponential diodes and two resistors, one is parallel and the other one is in series with the generated current as shown in Fig. 8.

The output current of the solar cell can be computed by [17–19]:

$$i = i_{\mathrm{ph}} - i_{o1} \cdot \left(e^{\frac{v + i \cdot Rs}{a_1 \cdot v_t}} - 1 \right) - i_{o2} \cdot \left(e^{\frac{v + i \cdot Rs}{a_2 \cdot v_t}} - 1 \right) - \frac{v + i \cdot R_s}{R_p} \tag{15}$$

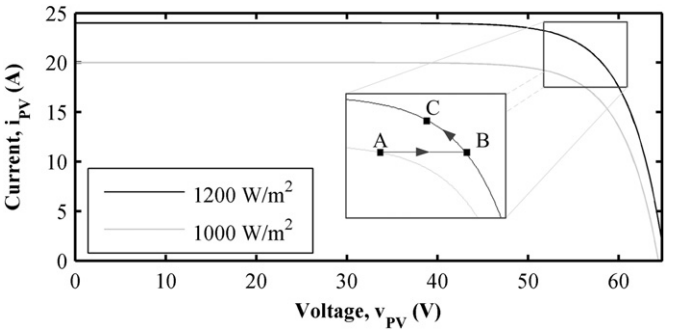

Fig. 9. I–V characteristics of the PV system for two different irradiance levels with marked respective maximum power points A and B for 1000 and 1200 W/m^2, respectively.

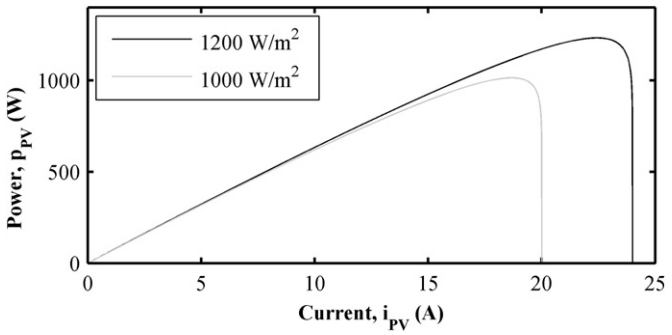

Fig. 10. *P–I* characteristics of the PV system for two different irradiance levels.

where i_{ph} is the photovoltaic current generated by solar irradiation, i_{o1}, i_{o2} are the *D*1, *D*2 reverse saturation currents, a_1, a_2 are the diode ideal constants, v_t is the thermal voltage and v is the terminal voltage. In case of the parallel and series combination of solar cells, i_{ph}, i_{o1}, i_{o2} can be multiplied by N_P and v_t by N_S, where N_P and N_S are the parallel and series connection of cells, respectively.

From the evaluation of (15), *I–V* characteristics of the examined PV system configuration for two different values of irradiance level, 1000 and 1200 W/m^2, can be obtained as shown in Fig. 9.

With letter *A* is marked the MPP of the *I–V* characteristic for solar radiation equal to 1000 W/m^2. Under an abrupt change in solar radiation from 1000 to 1200 W/m^2 the system is expected to operate, after the MPPT contribution, at point *C*, which is the MPP for 1200 W/m^2 solar irradiance. PV system current (i_{PV}) at point *A* and *C* is 18.6 and 22.3 A, respectively.

Fig. 10 shows the *P–I* characteristic of the PV system for the two aforementioned solar radiation levels, where the respective MPPs can be easily observed.

4.2. Investigation among the presented approaches

In the proposed control methodology, MPPT reference output constitutes the real time input in the predictive controller. The controller provided with the computed reference output (i^*) by the MPPT operates suitably the boost converter switch considering two-step horizon prediction in one sampling period. Contrarily, the PI controller demands sufficient time for the system to reach steady state operation, increasing time interval between two successive reference outputs from the MPPT and thus deteriorating system dynamic performance under abrupt and continuous variations.

In order to illustrate the benefits from the proposed control technique three different approaches are examined under solar irradiance variations: conventional approach (PI controller interacts with the traditional MPPT requiring sufficient time interval), the simplified MPC (MPC is configured as the conventional approach) and the proposed MPC (real time interaction between the modified MPPT and the MPC). Table 1 summarizes the main characteristics of the compared methodologies.

Table 1
Characteristics of the presented approaches.

	Conventional approach	Simplified MPC	Proposed MPC
Controller type	PI controller	MPC	MPC
Interaction with MPPT	$t_{interval}$	$t_{interval}$	T_s
Reference current $i^*_{(t+1)}$	$i^*_{(t)} + i_{inc}$	$i^*_{(t)} + i_{inc}$	$i_{PV(t)} + i_{inc}$
MPPT increment		i_{inc}	
System parameters		Same	

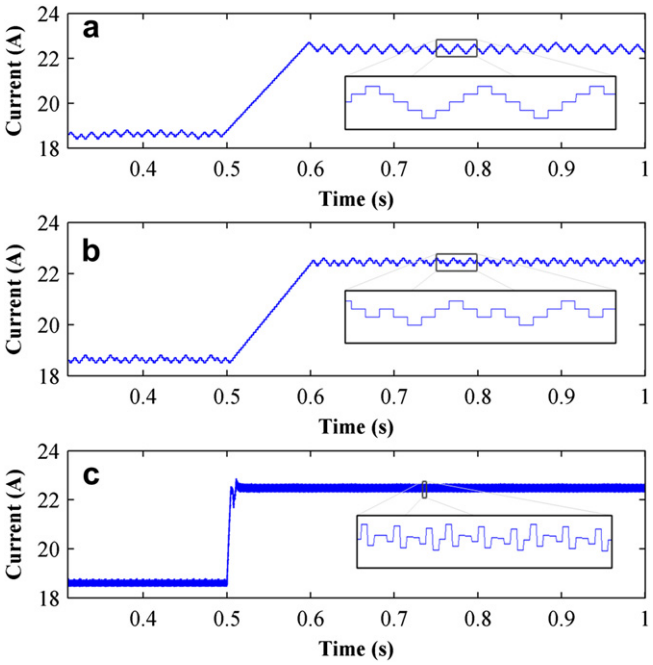

Fig. 11. MPPT output reference current (i^*) under irradiance variation from 1000 to 1200 W/m^2 for each different approach. (a) Conventional approach. (b) Simplified MPC. (c) Proposed MPC.

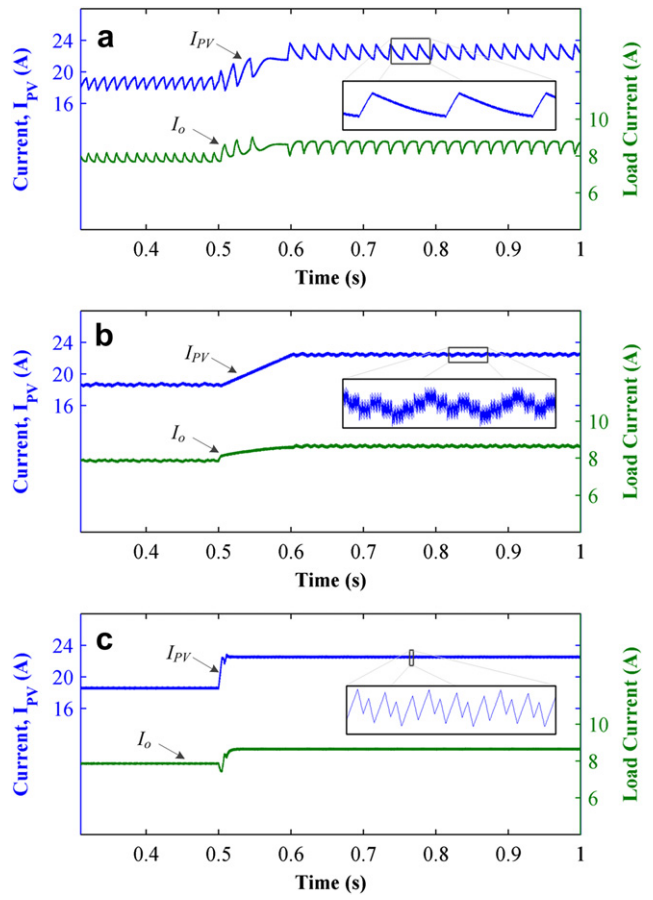

Fig. 12. PV system output current (i_{PV}) under irradiance variation from 1000 to 1200 W/m^2 for each different approach. (a) Conventional approach. (b) Simplified MPC. (c) Proposed MPC.

4.2.1. System behavior under abrupt solar irradiance variation

Presented approaches have been tested under an abrupt increase of solar radiation by 20% examining transient behavior and maximum energy exploitation. Fig. 11 shows MPPT output references (i^*) for the three different approaches. The conventional technique and the simplified MPC are not capable of following rapidly the change in solar radiation because of the required time interval for the system to remain stable.

Furthermore, oscillations around the MPP can be observed for these two approaches, but not with the same intensity for the simplified MPC. Conventional approach for the same system settings presents oscillations due to system delay to reach steady state operation. PI gains adopted have been obtained from different simulations carried out as the most appropriate for this system configuration.

In contrast, the proposed MPC due to the real time interaction with the MPPT presents advantages over the conventional techniques tracking the MPP with significantly increased speed and thus saving power energy. Fig. 12 shows that the output PV system current (i_{PV}) follows accurately the reference currents for the methods involved MPC.

The mathematical character of the MPC enables system to behave the same way under any transient phenomenon tracking accurately the MPP, and does not necessitate the reevaluation of control system parameters. Contrarily, through PI controller it is possible to present steady state error, due to the fact that the PI gains cannot guarantee same transient response under different system conditions keeping concurrently increased speed.

Fig. 13 depicts the produced power from the PV array and the total system output power. Total power dissipation comparing the three control schemes is higher for the conventional and simplified approach considering the time required for the system to reach MPP.

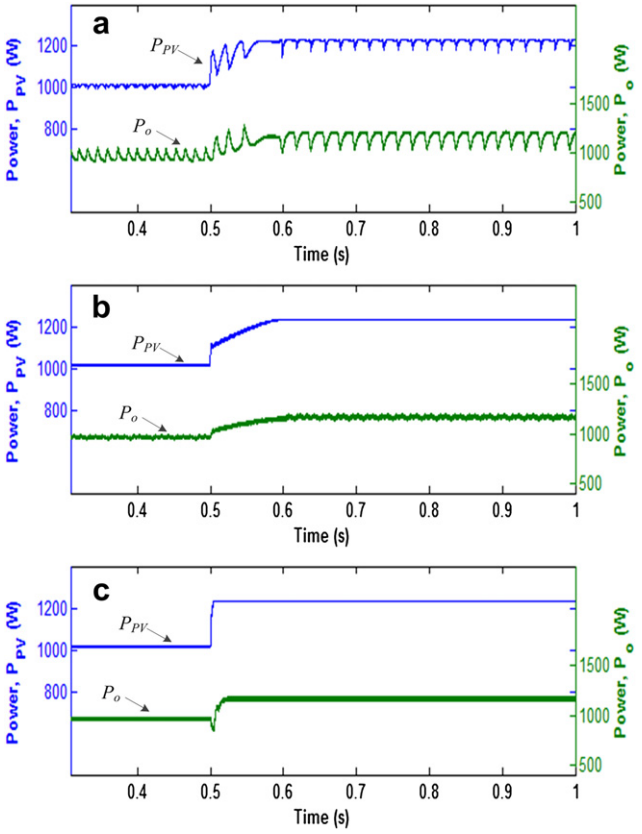

Fig. 13. Overall system generated power under irradiance variation from 1000 to 1200 W/m^2. (a) Conventional approach. (b) Simplified MPC. (c) Proposed MPC.

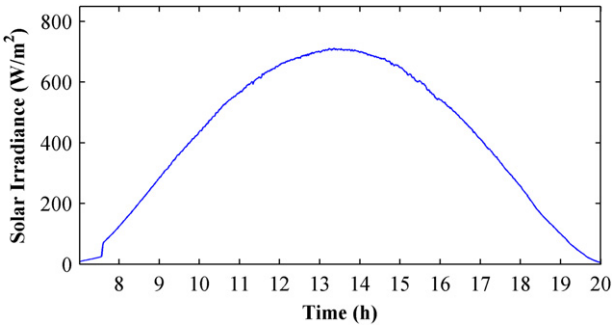

Fig. 14. Measured time series of the solar irradiance levels at NTUA campus (August 2010).

However, methods involving MPC, the simplified and the proposed method, as already mentioned, are not affected significantly from transient phenomena; though converge precisely and almost independently at the MPP. Considering the examined variation system achieve high level of MPPT efficiency of about 99.86%, while the conventional approach efficiency is of 99.36%, without considering power dissipation during transient response. The total amount of energy is significant assuming continuous operation all over the year.

4.2.2. Solar irradiance variations under various sky conditions

Previous analysis has shown that the proposed MPC is featured by its capability of achieving both better transient response and higher PV system utilization. In order to illustrate the effectiveness of the proposed control scheme real solar radiation data measured at the National Technical University Campus in Athens (NTUA), have been employed.

Measurements of solar irradiance levels under three different weather conditions have been carried out. Fig. 14 depicts the measured time series of the solar radiation for a sunny day without the presence of clouds and, therefore, the differentiation of the three presented control schemes is marginal.

Figs. 15 and 16 show the measured time series of the solar irradiance levels under the sporadic presence of clouds. Under cloudy sky conditions solar radiation fluctuates with abrupt changes necessitating the MPPT control to be reliable and accurate overcoming such difficulties and disturbances and increasing system conversion efficiency. Fig. 16 refers to a winter day where the solar irradiance levels are significantly low.

The results derived from the solar radiation data reveal that the proposed MPC achieves conversion system efficiency of about

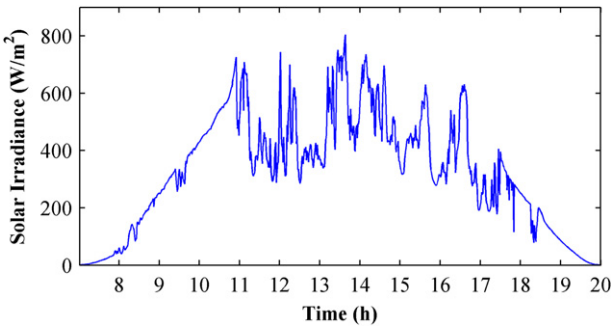

Fig. 15. Measured time series of the solar irradiance levels at NTUA campus (April 2010).

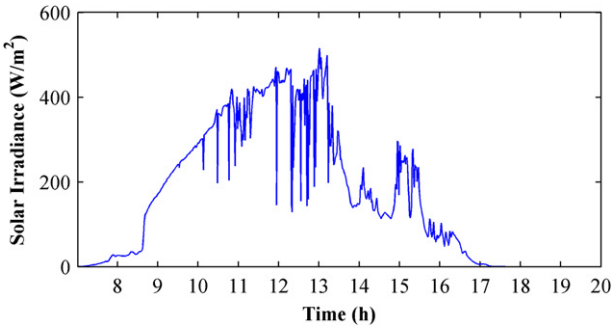

Fig. 16. Measured time series of the solar irradiance levels at NTUA campus (December 2009).

95.7% compared to the maximum energy exploitation, while the simplified approach attains lower efficiency of 94.1% considering a cloudy day as the solar radiation data employed.

5. Conclusions

This study focuses on the controller technique in order to attain maximum energy exploitation by applying modifications to one of the most widely used MPPT, thus a PV array MPPT through predictive control technique has been developed. The capacity of the MPC of being supplied with the reference current by the MPPT at one sampling time enables high transient response under abrupt changes in solar irradiance, presented usually under cloudy sky conditions. Solar irradiance varies continuously and abruptly under such sky conditions necessitating methods for harnessing maximum energy considering operation all over the year. Proposed control scheme efficiency has been illustrated by employing real solar radiation data into the simulation model.

Appendix. Table S1 summarizes main specifications for the examined PV system configuration.

Table S1
Main system specifications.

Inductance, L (mH)	20
Capacitance, C (μF)	50
MPPT increment (mA)	100
Time interval (MPPT) (ms)	0.5
Time interval (MPC) (μs)	50
Sampling time, T_s (μs)	50

References

[1] Houssamo I, Locment F, Sechilariu M. Maximum power tracking for photovoltaic power system: development and experimental comparison of two algorithms. Renewable Energy 2010;35:2381–7.
[2] Masoum M, Dehbonei H, Fuchs E. Theoretical and experimental analyses of photovoltaic systems with voltage and current-based maximum power-point tracking. IEEE Transactions On Energy Conversion 2002;17:514–22.
[3] Ropp ME, Gonzalez S. Development of a MATLAB/Simulink model of a single-phase grid-connected photovoltaic system. IEEE Transactions On Energy Conversion 2009;24:195–202.
[4] Pandey A, Dasgupta N, Mukerjee AK. High-performance algorithms for drift avoidance and fast tracking in solar MPPT system. IEEE Transactions On Energy Conversion 2008;23:681–9.
[5] Pan C, Juan Y. A novel sensorless MPPT controller for a high-efficiency microscale wind power generation system. IEEE Transactions On Energy Conversion 2010;25:207–16.
[6] Chiu C. T–S fuzzy maximum power point tracking control of solar power generation systems. IEEE Transactions On Energy Conversion; 2010:1–10.
[7] Gounden N, Annpeter S, Nallandula H, Krithiga S. Fuzzy logic controller with MPPT using line-commutated inverter for three-phase grid-connected photovoltaic systems. Renewable Energy 2009;34:909–15.
[8] Larbes C, Aït Cheikh S, Obeidi T, Zerguerras A. Genetic algorithms optimized fuzzy logic control for the maximum power point tracking in photovoltaic system. Renewable Energy 2009;34:2093–100.
[9] Chen L, Tsai C, Lin Y, Lai Y. A biological swarm chasing algorithm for tracking the PV maximum power point. IEEE Transactions On Energy Conversion 2010;25:484–93.
[10] Syafaruddin, Karatepeb E, Hiyamaa T. Polar coordinated fuzzy controller based real-time maximum-power point control of photovoltaic system. Renewable Energy 2009;34:2597–606.
[11] Salas V, Alonso-Abellá M, Chenlo F, Olías E. Analysis of the maximum power point tracking in the photovoltaic grid inverters of 5 kW. Renewable Energy 2009;34:2366–72.
[12] Cortés P, Kazmierkowski MP, Kennel RM, Quevedo DE, Rodríguez J. Predictive control in power electronics and drives. IEEE Transactions On Industrial Electronics 2008;55:4312–24.
[13] Kouro S, Cortes P, Vargas R, Ammann U, Rodriguez J. Model predictive control—a simple and powerful method to control power converters. IEEE Transactions On Industrial Electronics 2009;56:1826–38.
[14] Khalid M, Savkin A. A model predictive control approach to the problem of wind power smoothing with controlled battery storage. Renewable Energy 2010;35:1520–6.
[15] Hua C, Wu C, Chuang C. A digital predictive current control with improved sampled inductor current for cascaded inverters. IEEE Transactions On Industrial Electronics 2009;56:1718–26.
[16] Teng T-P, Nieh H-M, Chen J-J, Lu Y-C. Research and development of maximum power transfer tracking system for solar cell unit by matching impedance. Renewable Energy 2010;35:845–51.
[17] Villalva MG, Gazoli JR, Filho ER. Comprehensive approach to modeling and simulation of photovoltaic arrays. IEEE Transactions On Power Electronics 2009;24:1198–208.
[18] Andrade Da Costa B, Lemos J. An adaptive temperature control law for a solar furnace. Control Engineering Practice 2009;17:1157–73.
[19] Armstrong S, Hurley WG. A new methodology to optimise solar energy extraction under cloudy conditions. Renewable Energy 2010;35:780–7.